

Supporting Information

Non-Stoichiometry as a Structural Lever: Tailoring Oxygen Sublattice Occupancy for Enhanced Oxide-Ion Transport in BIVCUOX

Wei-Xin Yan^a, Dong-Mei Zhu^a, Ke Shu^a, Huai-Hai Li^a, Lei-Ming Fang^b, Chun-Hai Wang^{a,*}

^aState Key Laboratory of Solidification Processing, Northwestern Polytechnical University, Xi'an, Shaanxi 710072, China

^bKey Laboratory for Neutron Physics, Institute of Nuclear Physics and Chemistry, China Academy of Engineering Physics, Mianyang 621900, People's Republic of China

* Corresponding author, email: chwang81@gmail.com

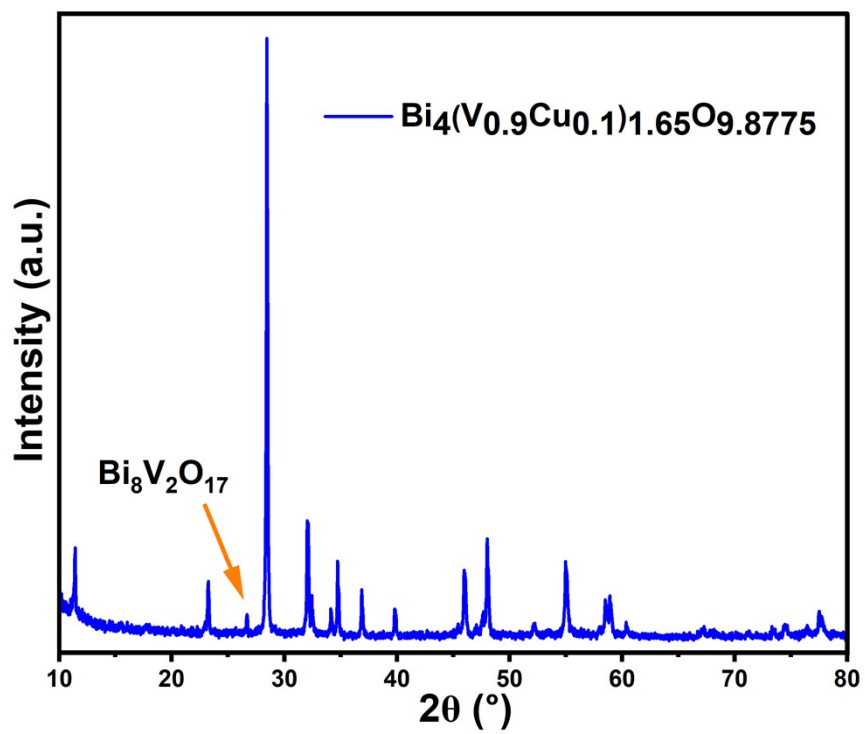


Fig.S1 The XRD pattern of $\text{Bi}_4(\text{V}_{0.9}\text{Cu}_{0.1})_{1.65}\text{O}_{9.8775}$

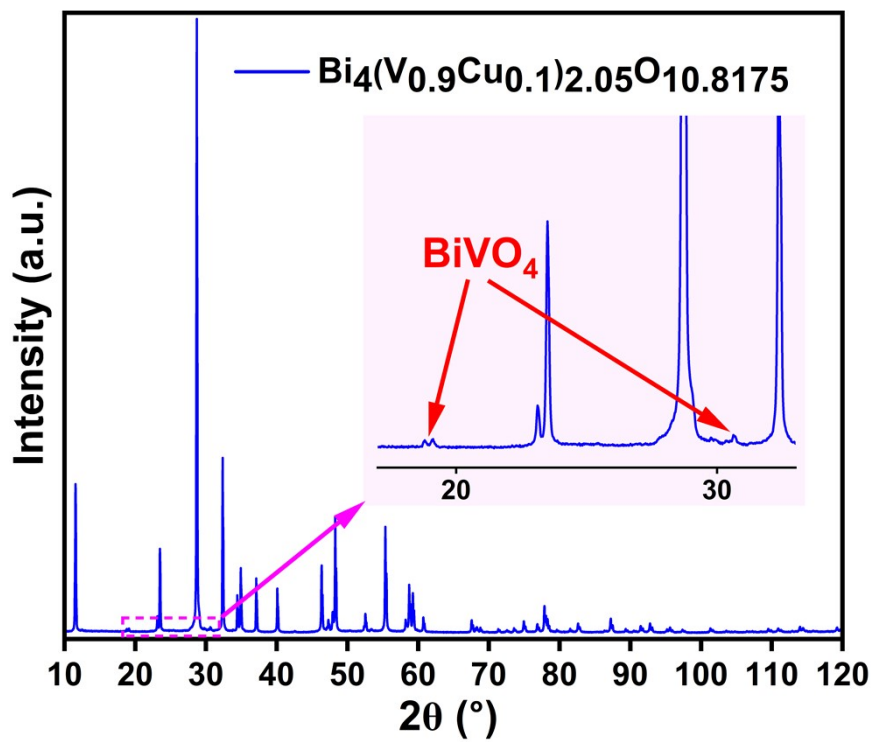


Fig.S2 The XRD pattern of $\text{Bi}_4(\text{V}_{0.9}\text{Cu}_{0.1})_{2.05}\text{O}_{10.8175}$

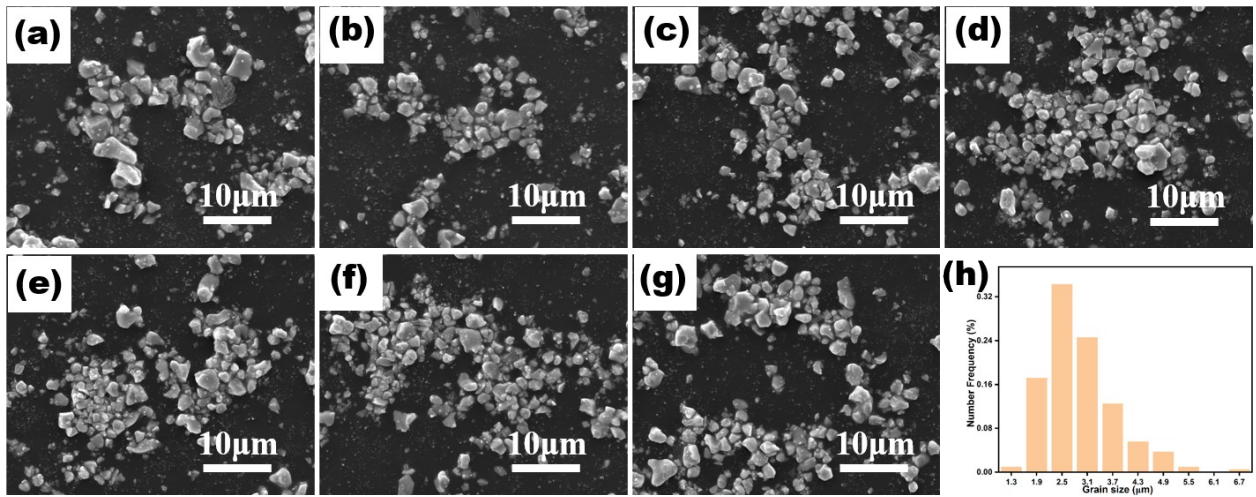


Fig. S3 (a – g) SEM images of $\text{Bi}_4(\text{V}_{0.9}\text{Cu}_{0.1})_x\text{O}_{6+2.35x}$ ($1.70 \leq x \leq 2.00$) powders; (h) The distribution of powder size of $\text{Bi}_4(\text{V}_{0.9}\text{Cu}_{0.1})_x\text{O}_{6+2.35x}$

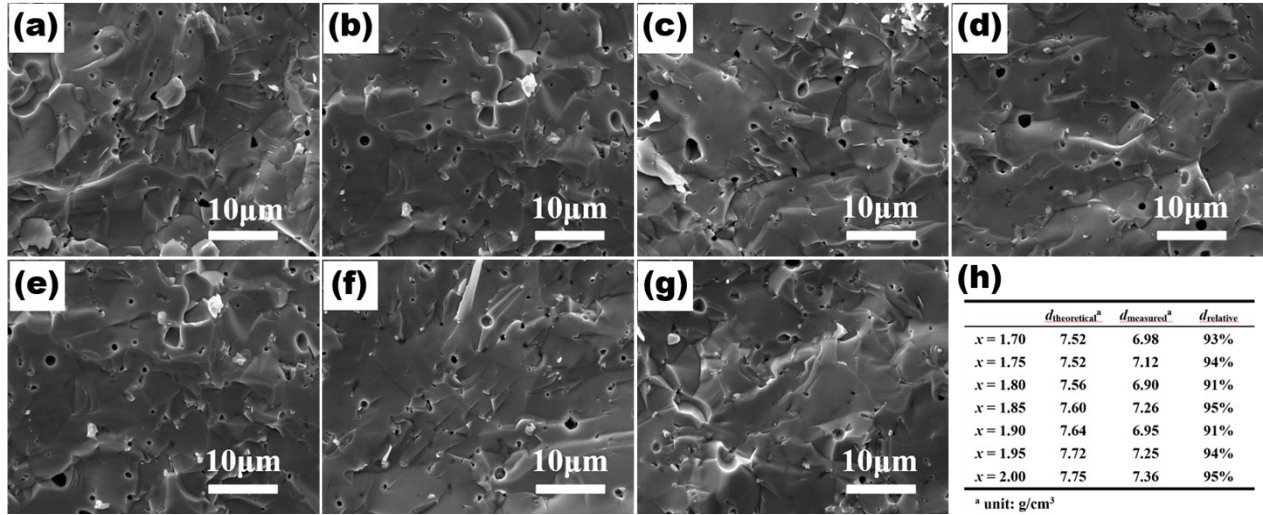


Fig. S4 (a – g) SEM images of Bi₄(V_{0.9}Cu_{0.1})_xO_{6+2.35x} ($1.70 \leq x \leq 2.00$) fractured surface of ceramics; (h) The theoretical, measured and relative density of Bi₄(V_{0.9}Cu_{0.1})_xO_{6+2.35x}

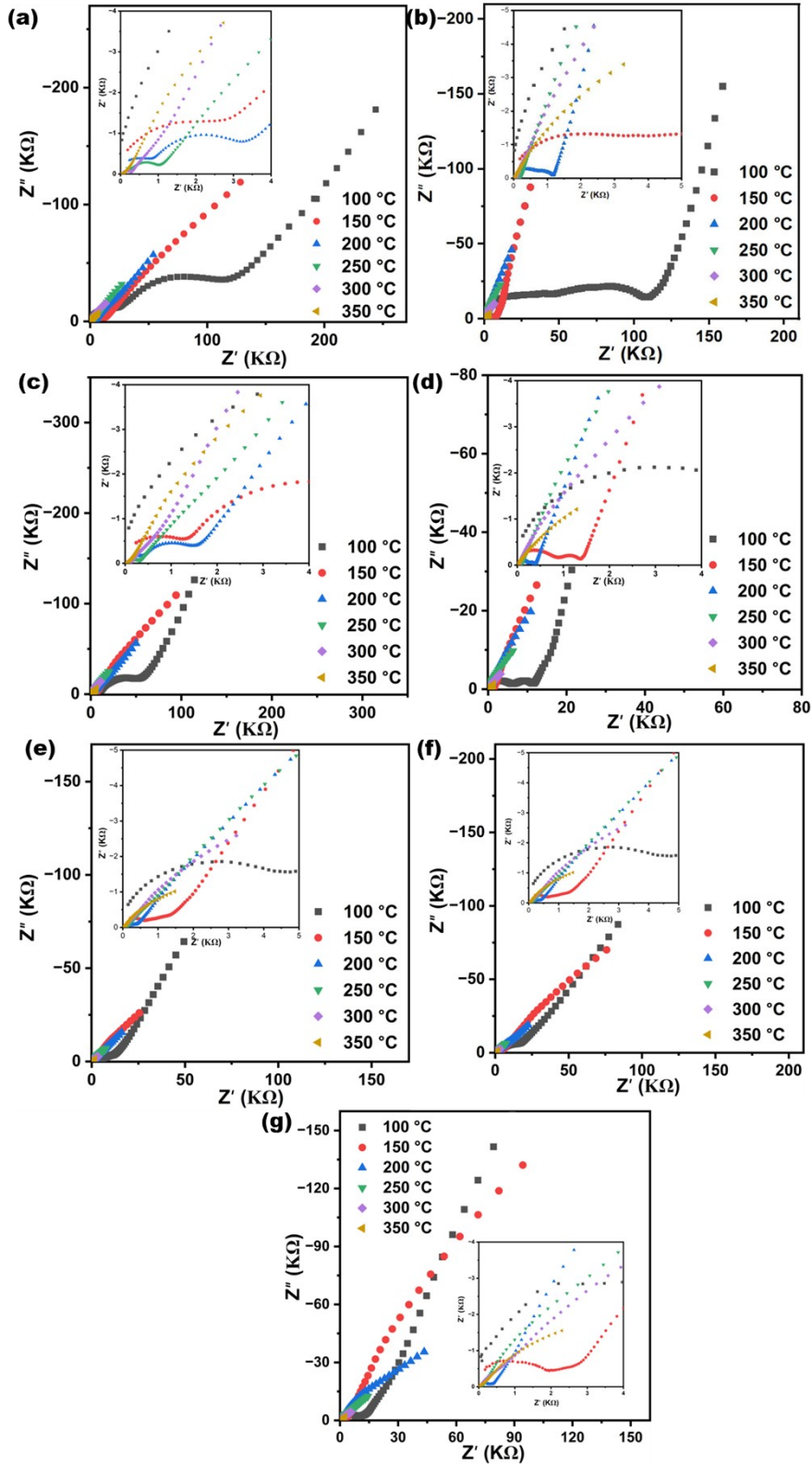


Fig. S6 Nyquist plots of $\text{Bi}_4(\text{V}_{0.9}\text{Cu}_{0.1})_x\text{O}_{6+2.35x}$ ($1.70 \leq x \leq 2.00$) (a) $x = 1.70$; (b) $x = 1.75$; (c) $x = 1.80$; (d) $x = 1.85$; (e) $x = 1.90$; (f) $x = 1.95$ and (g) $x = 2.00$

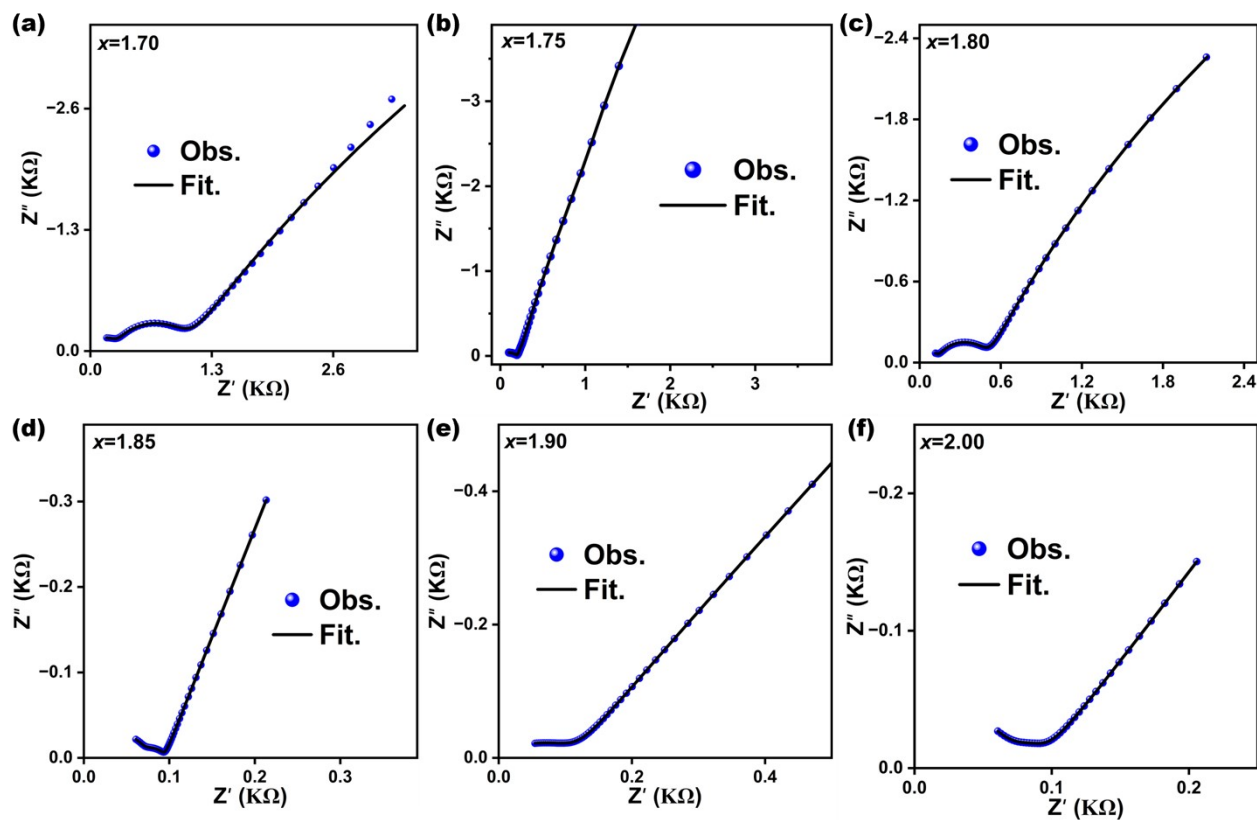


Fig. S7 The Nyquist plot of $\text{Bi}_4(\text{V}_{0.9}\text{Cu}_{0.1})_x\text{O}_{6+2.35x}$ ($1.75 \leq x \leq 2.00$) recorded at 250°C (a) $x = 1.75$; (b) $x = 1.80$; (c) $x = 1.85$; (d) $x = 1.90$; (e) $x = 1.95$; (f) $x = 2.00$. The black line and blue circles denote the fit to the data and experimental data, respectively.

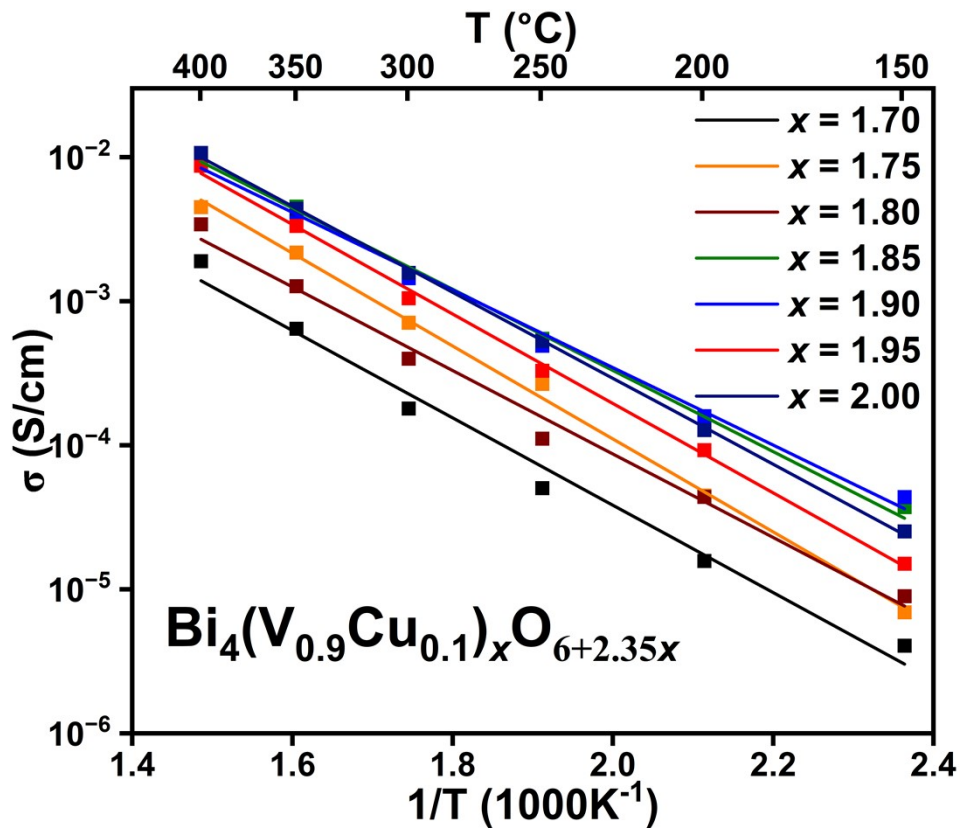


Fig. S8 The total conductivity of $\text{Bi}_4(\text{V}_{0.9}\text{Cu}_{0.1})_x\text{O}_{6+2.35x}$ ($1.70 \leq x \leq 2.00$)

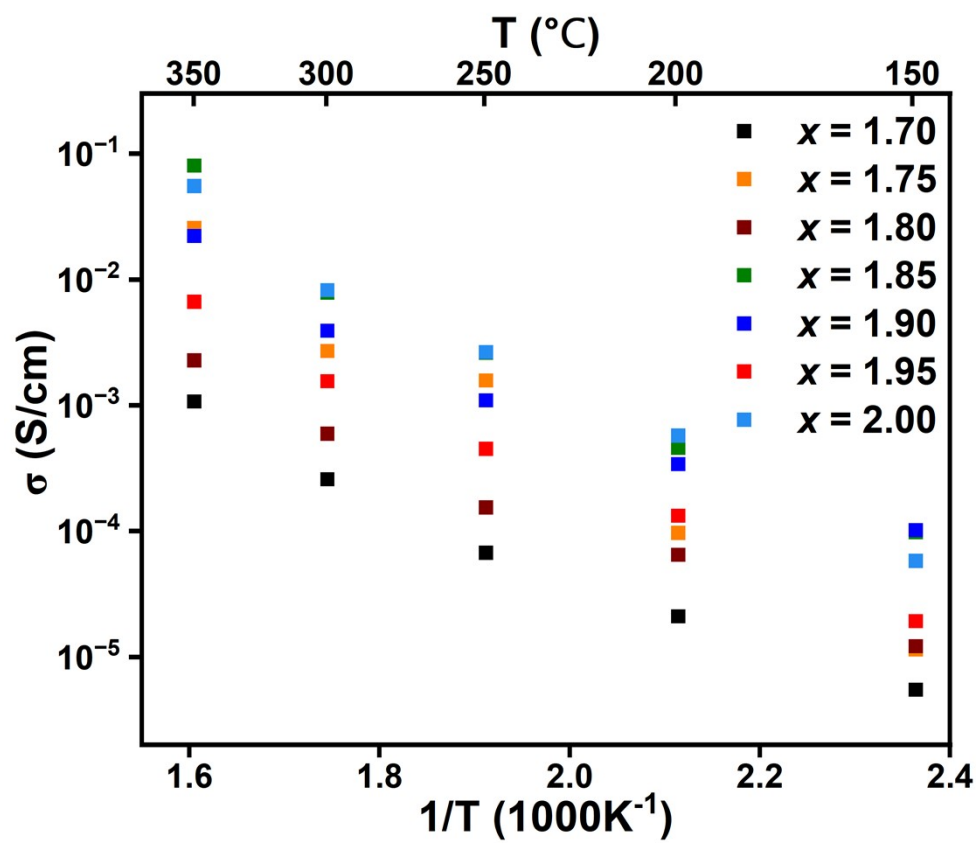


Fig. S9 The grain boundary conductivity of $\text{Bi}_4(\text{V}_{0.9}\text{Cu}_{0.1})_x\text{O}_{6+2.35x}$ ($1.70 \leq x \leq 2.00$)

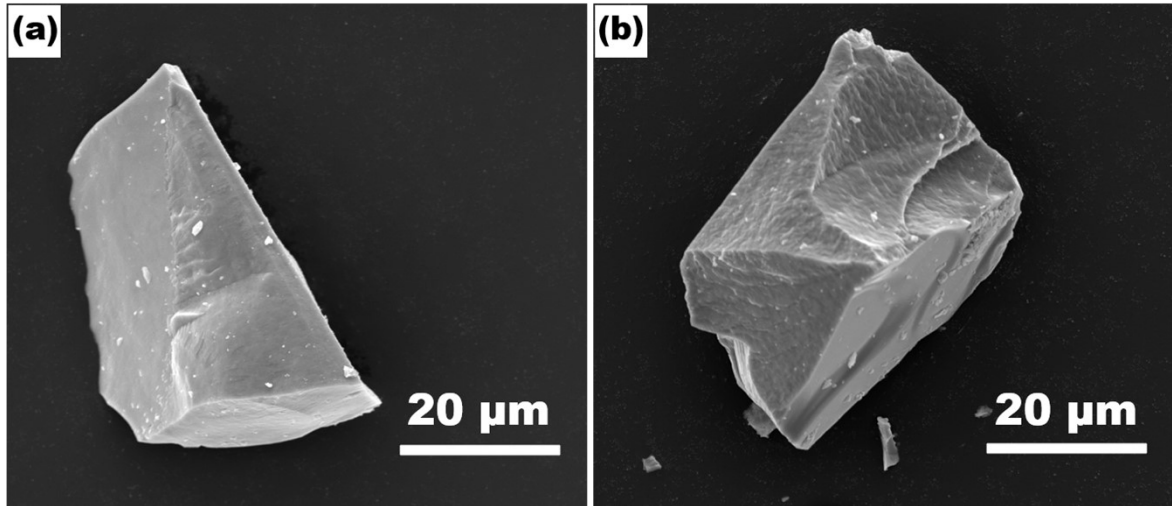


Fig. S10 The SEM images of $\text{Bi}_4(\text{V}_{0.9}\text{Cu}_{0.1})_{1.95}\text{O}_{10.5825}$ and $\text{Bi}_4(\text{V}_{0.9}\text{Cu}_{0.1})_{2.00}\text{O}_{10.7}$ microcrystal

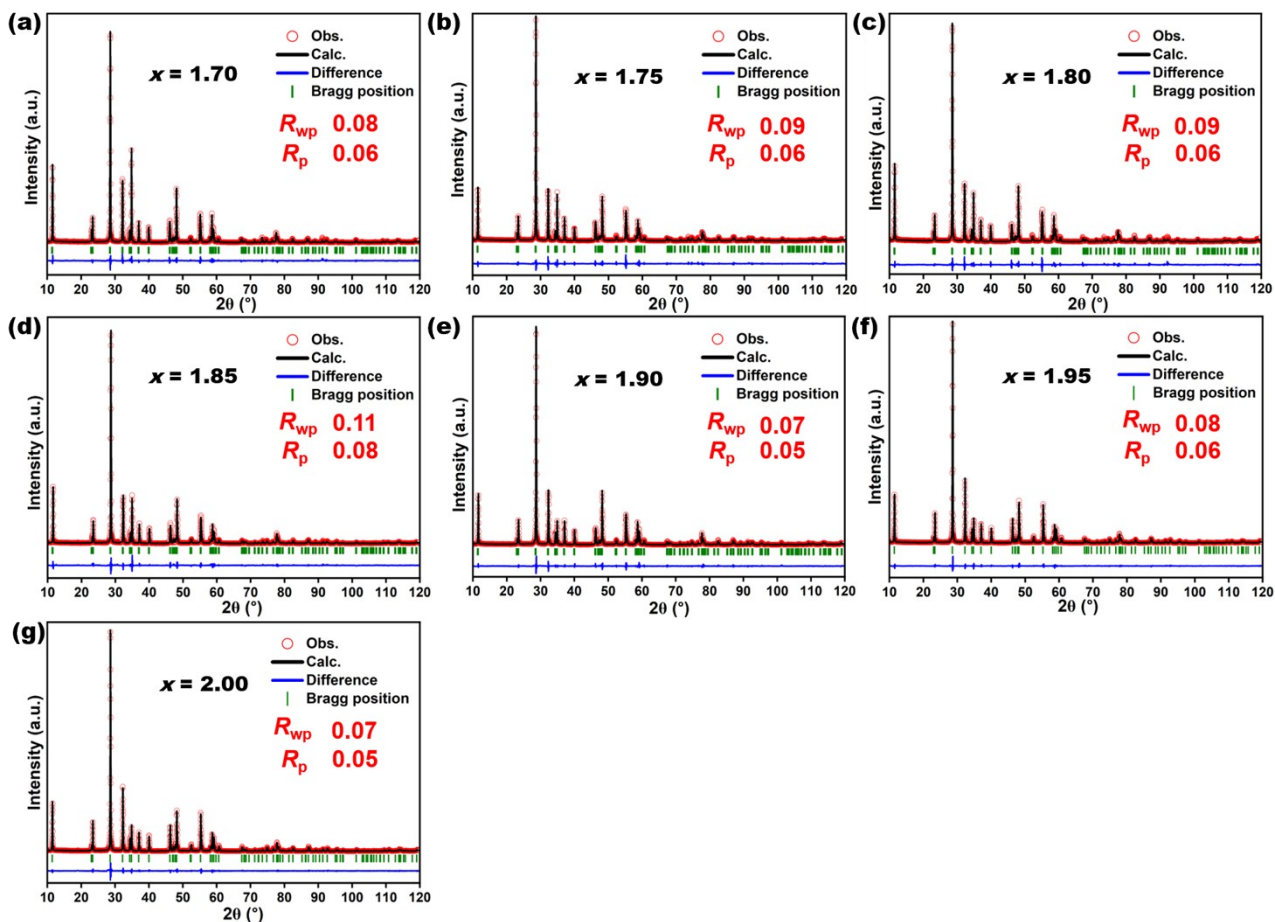


Fig. S11 Patterns of Rietveld refinement of $\text{Bi}_4(\text{V}_{0.9}\text{Cu}_{0.1})_x\text{O}_{6+2.35x}$ ($1.70 \leq x \leq 2.00$) obtained from PXRD. Red circles, black lines, blue lines, and green ticks represent observed, calculated, difference intensities, and Bragg peak positions, respectively.

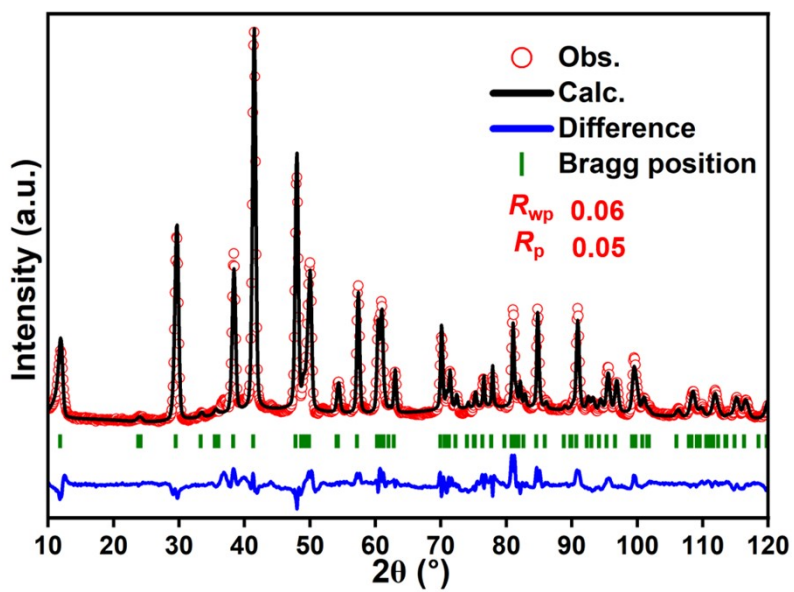


Fig. S12 Patterns of Rietveld refinement of $\text{Bi}_4(\text{V}_{0.9}\text{Cu}_{0.1})_{2.0}\text{O}_{10.7}$ obtained from PND. Red circles, black lines, blue lines, and green ticks represent observed, calculated, difference intensities, and Bragg peak positions, respectively.

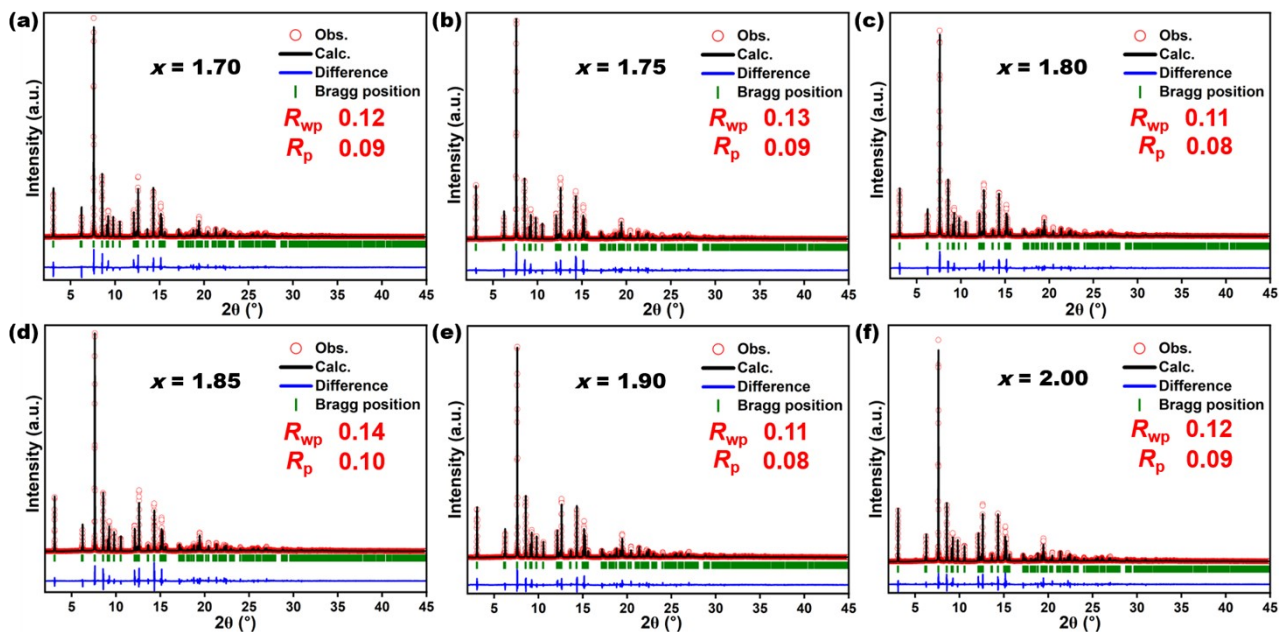


Fig. S13 Patterns of Rietveld refinement of $\text{Bi}_4(\text{V}_{0.9}\text{Cu}_{0.1})_x\text{O}_{6+2.35x}$ ($1.70 \leq x \leq 2.00$) ($x = 1.70$, $x = 1.75$, $x = 1.85$, $x = 1.90$ and $x = 2.00$) obtained from SRXRD. Red circles, black lines, blue lines, and green ticks represent observed, calculated, difference intensities, and Bragg peak positions, respectively.

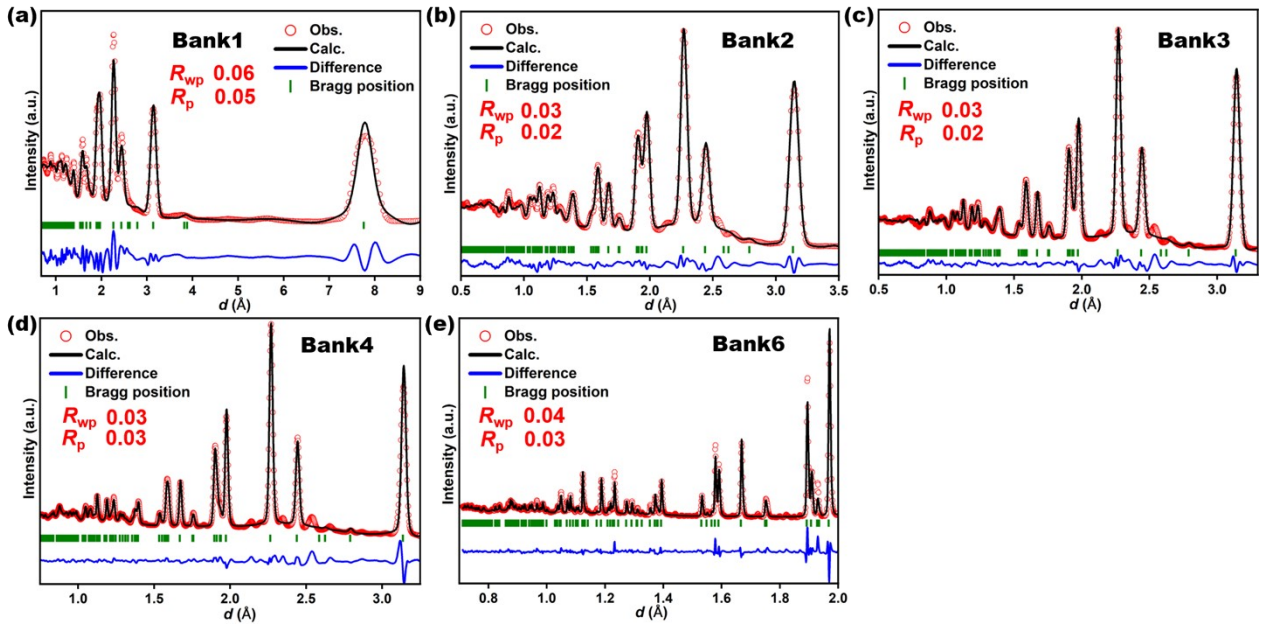


Fig. S14 Patterns of Rietveld refinement of $\text{Bi}_4(\text{V}_{0.9}\text{Cu}_{0.1})_{1.95}\text{O}_{10.5825}$ obtained from TOF. (a) Bank1 ($d = 0.6 - 9.0$ Å); (b) Bank2 ($d = 0.5 - 3.5$ Å); (c) Bank3 ($d = 0.5 - 3.3$ Å); (d) Bank4 ($d = 0.7 - 3.2$ Å); (e) Bank6 ($d = 0.7 - 2.0$ Å). Red circles, black lines, blue lines, and green ticks represent observed, calculated, difference intensities, and Bragg peak positions, respectively.

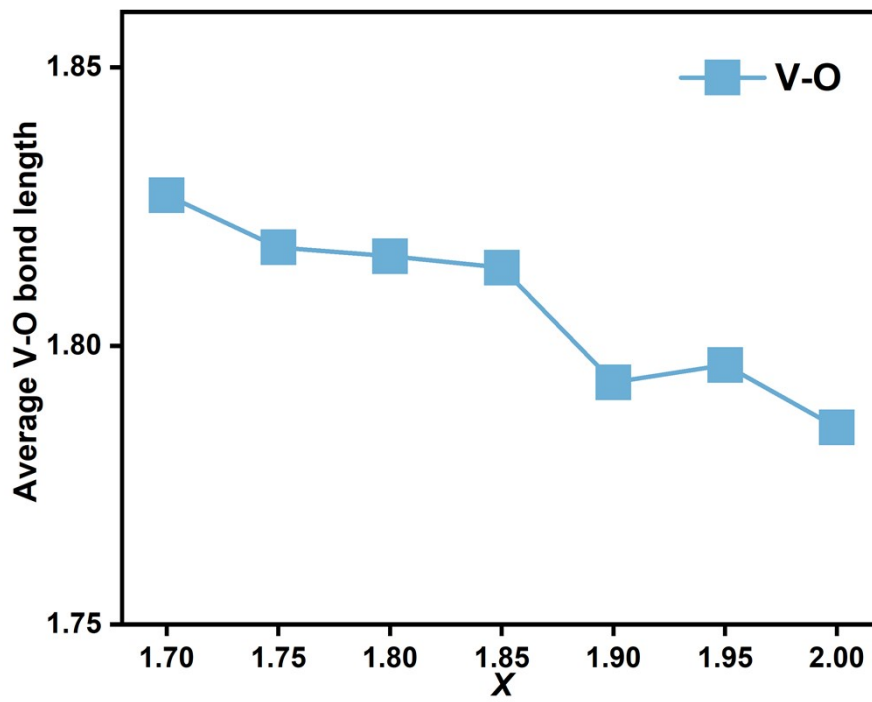


Fig. S15 The average bond length of V-O of $\text{Bi}_4(\text{V}_{0.9}\text{Cu}_{0.1})_x\text{O}_{6+2.35x}$ ($1.70 \leq x \leq 2.00$)

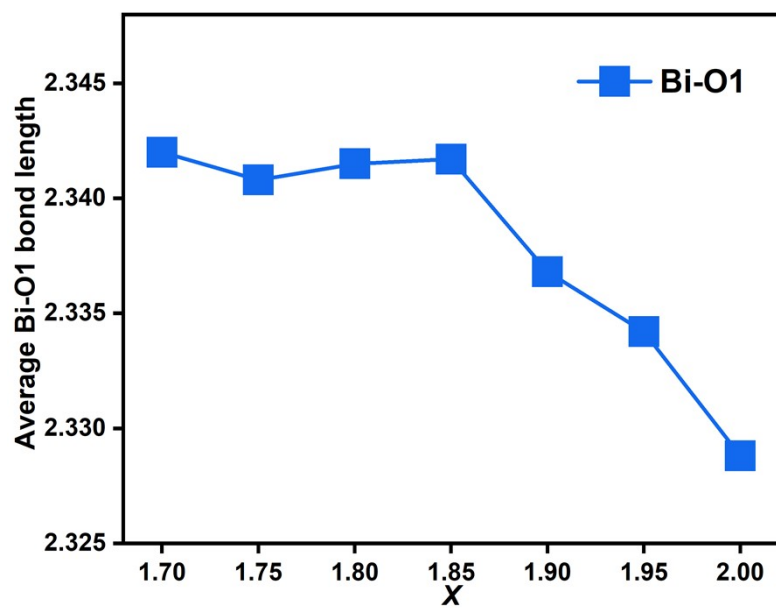


Fig. S16 The average bond length of Bi-O of $\text{Bi}_4(\text{V}_{0.9}\text{Cu}_{0.1})_x\text{O}_{6+2.35x}$ ($1.70 \leq x \leq 2.00$)

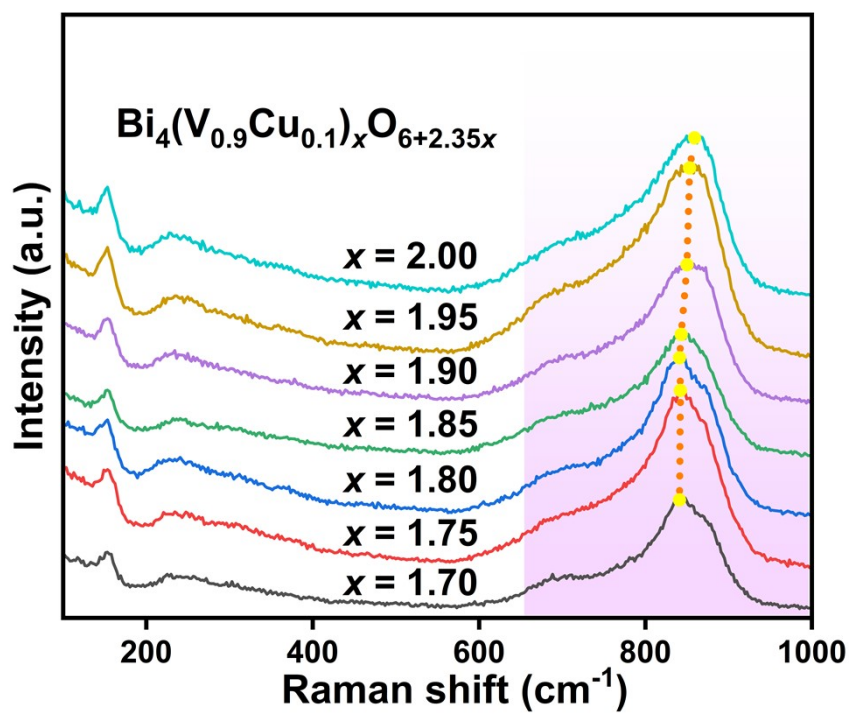


Fig. S17 The Raman spectra of $\text{Bi}_4(\text{V}_{0.9}\text{Cu}_{0.1})_x\text{O}_{6+2.35x}$ ($1.70 \leq x \leq 2.00$)

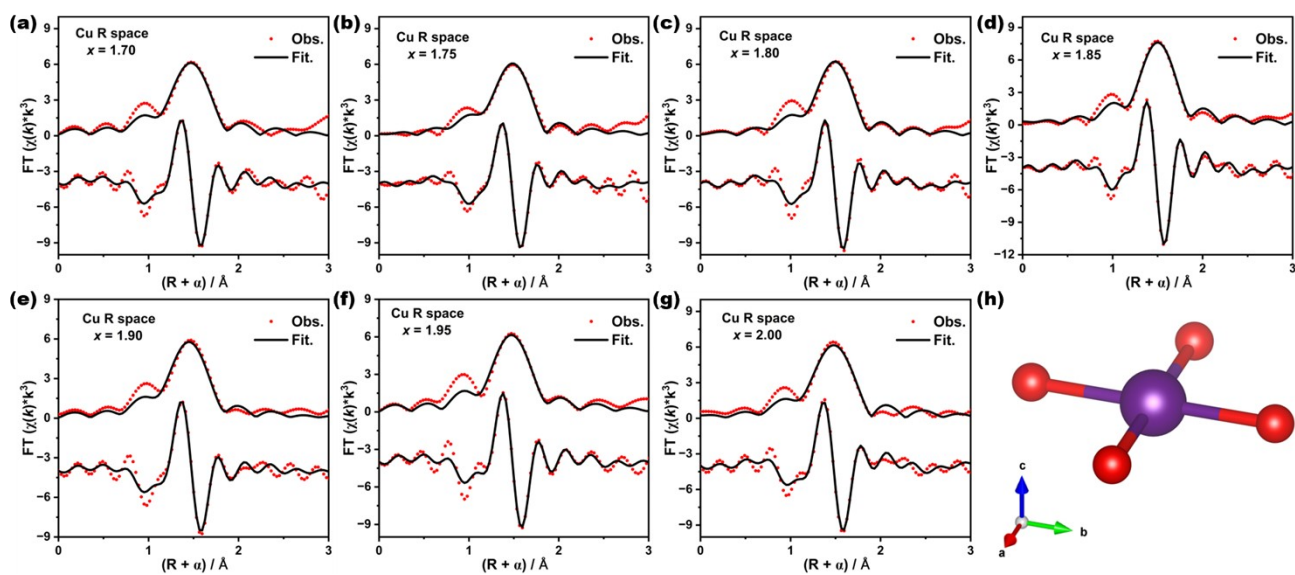


Fig. S18 Cu-edge EXAFS of $\text{Bi}_4(\text{V}_{0.9}\text{Cu}_{0.1})_x\text{O}_{6+2.35x}$ ($1.70 \leq x \leq 2.0$) in non-phase-corrected R-space ((FT magnitude and its imaginary component, red points); (h) The structure represents refinement to the first-coordination sphere of a Cu–O model.

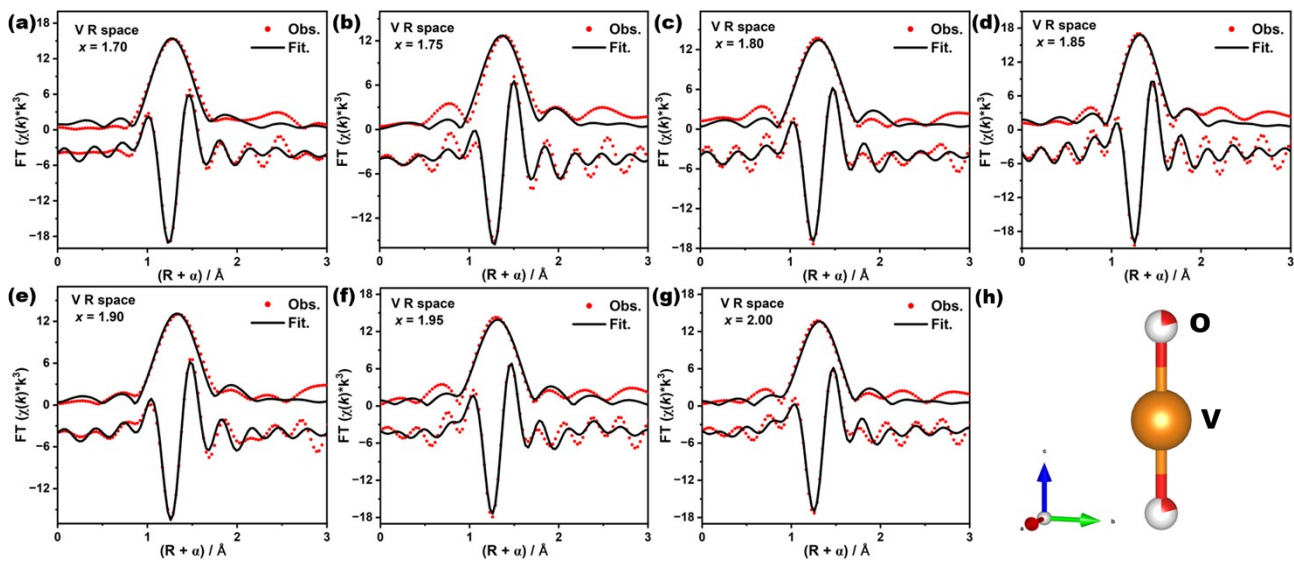


Fig. S19 V-edge EXAFS of $\text{Bi}_4(\text{V}_{0.9}\text{Cu}_{0.1})_x\text{O}_{6+2.35x}$ ($1.70 \leq x \leq 2.0$) in non-phase-corrected R-space (FT magnitude and its imaginary component, red points)

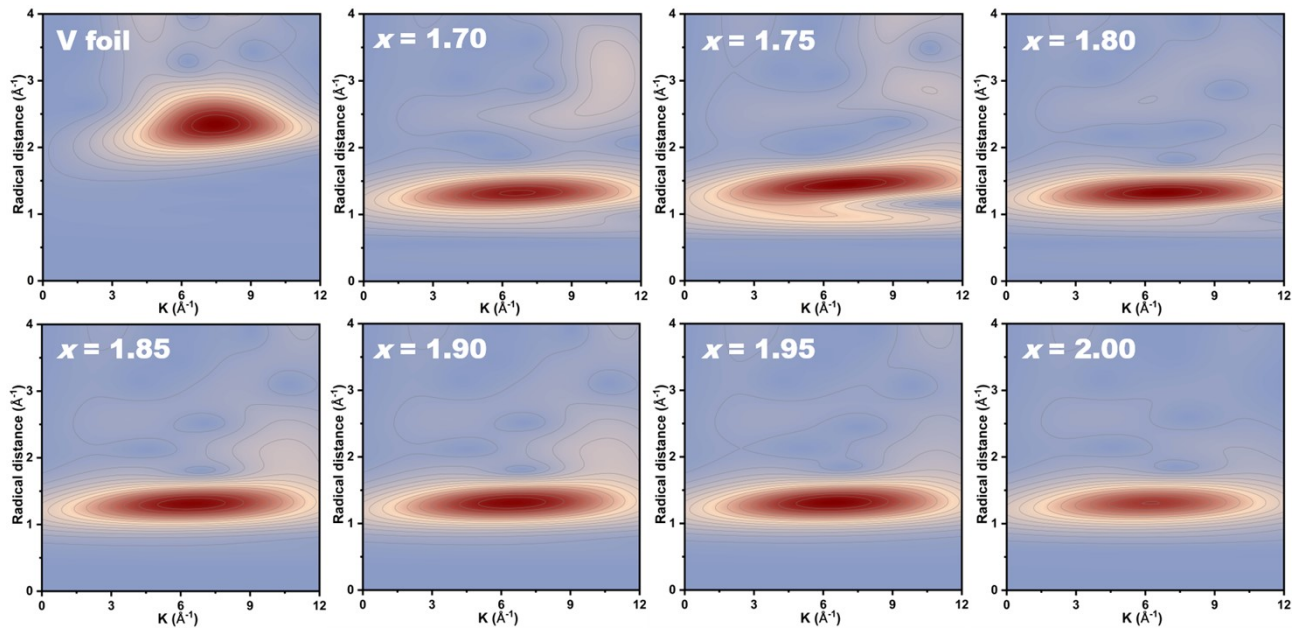


Fig. S20 Wavelet transforms of the k^3 -weighted V

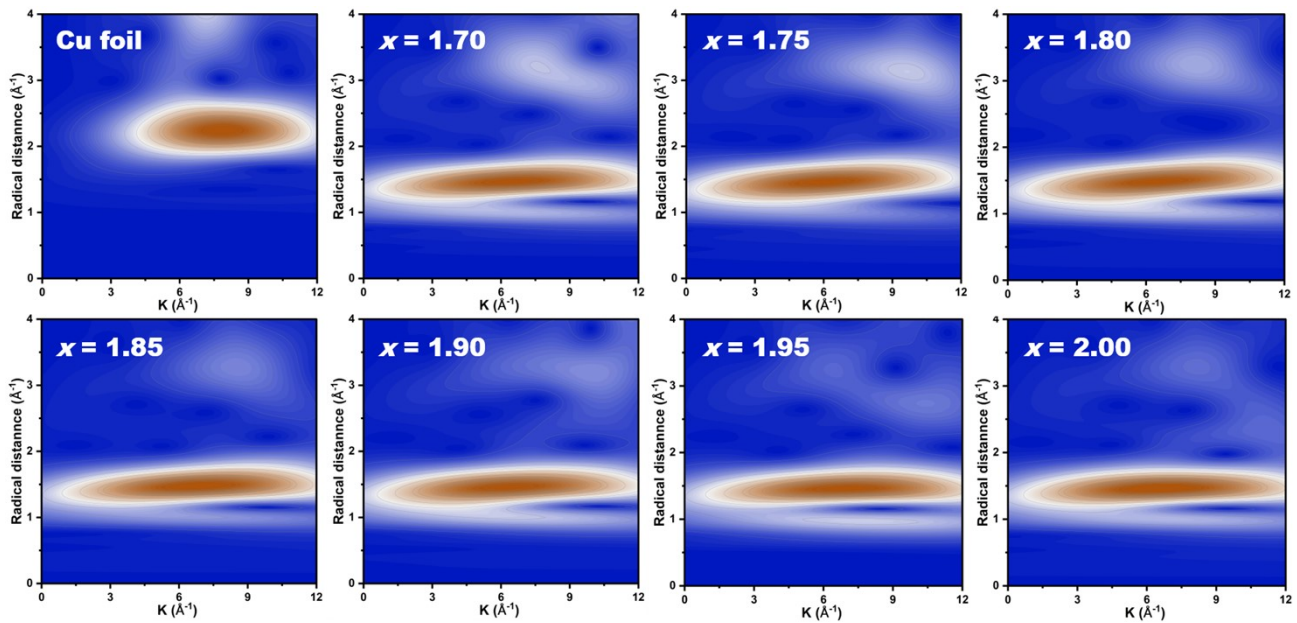


Fig. S21 Wavelet transforms of the k^3 -weighted Cu

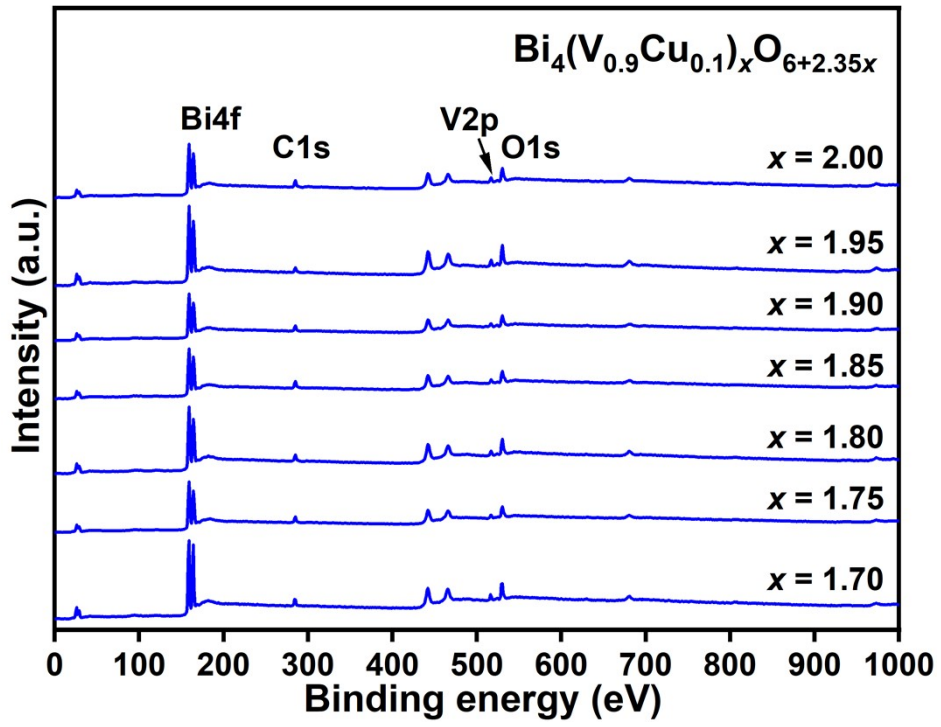


Fig. S22 The full XPS of $\text{Bi}_4(\text{V}_{0.9}\text{Cu}_{0.1})_x\text{O}_{6+2.35x}$ ($1.70 \leq x \leq 2.0$)

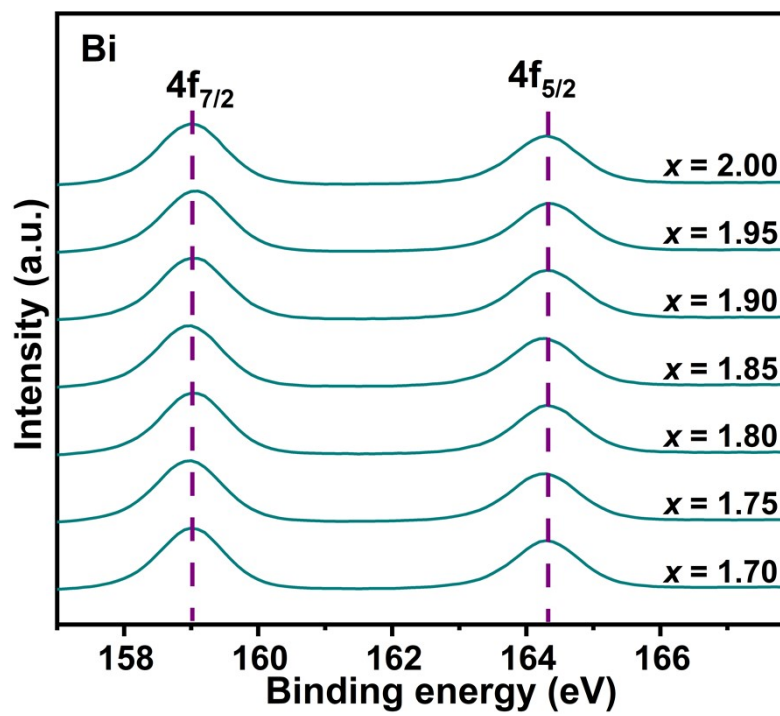


Fig. S23 High-resolution XPS of Bismuth 4f

Table S1 Grain and total ionic conductivity and activation energy of ns-BICUVOX

Samples	Grain	Total
	E_a (eV)	E_a (eV)
$x = 1.70$	0.52(2)	0.60(2)
$x = 1.75$	0.55(2)	0.64(2)
$x = 1.80$	0.51(2)	0.57(2)
$x = 1.85$	0.49(2)	0.55(2)
$x = 1.90$	0.47(2)	0.53(2)
$x = 1.95$	0.53(2)	0.61(2)
$x = 2.00$	0.53(2)	0.59(2)

Table S2 The details of the crystal structure of $\text{Bi}_4(\text{V}_{0.9}\text{Cu}_{0.1})_{1.95}\text{O}_{10.5825}$ obtained from SXRD

$\text{Bi}_4(\text{V}_{0.9}\text{Cu}_{0.1})_{1.95}\text{O}_{10.5825}$ (from SXRD) ^a			
Space group		$I4/mmm$ (no.139)	
a (Å)		3.9211(3)	
c (Å)		15.4283(1)	
V (Å ³)		237.210(3)	
d_{theory} (g cm ⁻³)		7.7(1)	
Atom	Site	Coordinate	Occ.
Bi	4e	(0.5, 0.5, 0.1692(4))	1
V	2a	(0, 0, 0)	0.8775
Cu	2a	(0, 0, 0)	0.0975
O1	4d	(0.5, 0, 0.25)	1
O2	8g	(0, 0.5, 0.0302(2))	0.340(1)
O3	4e	(0.5, 0.5, 0.3926(1))	0.221(2)
O4	16n	(0.6752(1), 0.5, 0.5959(1))	0.186(2)

^a Measured temperature 150 KTable S3. The ADP for each site in $\text{Bi}_4(\text{V}_{0.9}\text{Cu}_{0.1})_{1.95}\text{O}_{10.5825}$ (unit: Å²)

	U_{11}	U_{22}	U_{33}	U_{12}	U_{13}	U_{23}
Bi	0.0245(2)	0.0245(2)	0.0163(2)	0	0	0
V/Cu	0.0434(1)	0.0434(1)	0.0112(1)	0	0	0
O1	0.0108(2)	0.0108(2)	0.0351(2)	0	0	0
O2	0.0657(2)	0.0624(2)	0.0752(2)	0	0	0
O3	0.0657(2)	0.0624(2)	0.0752(2)	0	0	0
O4	0.0657(2)	0.0624(2)	0.0752(2)	0	0	0

Table S4 The details of the crystal structure of $\text{Bi}_4(\text{V}_{0.9}\text{Cu}_{0.1})_{2.00}\text{O}_{10.7}$ obtained from SXRD

$\text{Bi}_4(\text{V}_{0.9}\text{Cu}_{0.1})_{2.00}\text{O}_{10.7}$ (from SXRD) ^a			
Space group		$I4/mmm$ (no.139)	
a (Å)		3.9205(3)	
c (Å)		15.4476(1)	
V (Å ³)		237.435(3)	
d_{theory} (g cm ⁻³)		7.7(1)	
Atom	Site	Coordinate	Occ.
Bi	4e	(0.5, 0.5, 0.1692(2))	1
V	2b	(0, 0, 0)	0.9
Cu	2b	(0, 0, 0)	0.1
O1	4d	(0.5, 0, 0.25)	1
O2	8g	(0, 0.5, 0.0343(2))	0.316(1)
O3	4e	(0.5, 0.5, 0.3974(2))	0.400(2)
O4	16n	(0.7594(2), 0.5, 0.5890(2))	0.160(2)

^a Measured temperature 150 KTable S5. The ADP for each site in $\text{Bi}_4(\text{V}_{0.9}\text{Cu}_{0.1})_{2.00}\text{O}_{10.7}$ (unit: Å²)

	U_{11}	U_{22}	U_{33}	U_{12}	U_{13}	U_{23}
Bi	0.0197(2)	0.0197(2)	0.0122(2)	0	0	0
Cu/V	0.0370(1)	0.0370(1)	0.0129(1)	0	0	0
O1	0.0048(2)	0.0048(2)	0.0223(2)	0	0	0
O2	0.0578(3)	0.0821(3)	0.0702(2)	0	0	0
O3	0.0578(3)	0.0821(3)	0.0702(2)	0	0	0
O4	0.0578(3)	0.0821(3)	0.0702(2)	0	0	0

Table S6 The details of the crystal structure of $\text{Bi}_4(\text{V}_{0.9}\text{Cu}_{0.1})_{1.7}\text{O}_{9.995}$ obtained from PXRD and SRXRD

$\text{Bi}_4(\text{V}_{0.9}\text{Cu}_{0.1})_{1.7}\text{O}_{9.995}$ (from PXRD and SRXRD)				
Space group		$I4/mmm$ (NO.139)		
a (Å)		3.9414(4)		
c (Å)		15.4758(1)		
V (Å ³)		240.410(2)		
d_{theory} (g cm ⁻³)		7.52(2)		
Atom	Site	Coordinate	Occ.	B_{iso} (Å ²)
Bi	4e	(0.5, 0.5, 0.1682(4))	1	2.3(1)
V	2a	(0, 0, 0)	0.765	0.1(1)
Cu	2a	(0, 0, 0)	0.085	0.1(1)
O1	4d	(0, 0.5, 0.25)	1	3.3(1)
O2	8g	(0.5, 0, 0.4797(2))	0.50(1)	8.0(1)
O3	4e	(0, 0, 0.1136(1))	0.10(1)	5.9(1)
O4	16n	(0.6379(2), 0.5, 0.6059(1))	0.10(1)	5.9(1)

Table S7 The details of the crystal structure of $\text{Bi}_4(\text{V}_{0.9}\text{Cu}_{0.1})_{1.75}\text{O}_{10.1125}$ obtained from PXRD

$\text{Bi}_4(\text{V}_{0.9}\text{Cu}_{0.1})_{1.75}\text{O}_{10.1125}$ (from PXRD)				
Space group		$I4/mmm$ (NO.139)		
a (Å)		3.9363(4)		
c (Å)		15.4719(1)		
V (Å ³)		239.733(2)		
d_{theory} (g cm ⁻³)		7.52(2)		
Atom	Site	Coordinate	Occ.	B_{iso} (Å ²)
Bi	4e	(0.5, 0.5, 0.1681(4))	1	2.4(1)
V	2a	(0, 0, 0)	0.7875	0.1(1)
Cu	2a	(0, 0, 0)	0.0875	0.1(1)
O1	4d	(0, 0.5, 0.25)	1	2.3(1)
O2	8g	(0.5, 0, 0.4797(2))	0.46	8.0(1)
O3	4e	(0, 0, 0.1123(1))	0.22	6.0(1)
O4	16n	(0.6352(2), 0.5, 0.6059(1))	0.08	6.0(1)

Table S8 The details of the crystal structure of $\text{Bi}_4(\text{V}_{0.9}\text{Cu}_{0.1})_{1.80}\text{O}_{10.23}$ obtained from PXRD and SRXRD

$\text{Bi}_4(\text{V}_{0.9}\text{Cu}_{0.1})_{1.80}\text{O}_{10.23}$ (from PXRD and SRXRD)				
Space group		$I4/mmm$ (NO.139)		
a (Å)		3.9391(4)		
c (Å)		15.4666(1)		
V (Å ³)		239.985(2)		
d_{theory} (g cm ⁻³)		7.56(2)		
Atom	Site	Coordinate	Occ.	B_{iso} (Å ²)
Bi	4e	(0.5, 0.5, 0.1681(4))	1	2.1(1)
V	2a	(0, 0, 0)	0.81	0.6(1)
Cu	2a	(0, 0, 0)	0.09	0.6(1)
O1	4d	(0, 0.5, 0.25)	1	4.0(1)
O2	8g	(0.5, 0, 0.4797(2))	0.50	8.0(1)
O3	4e	(0, 0, 0.1121(1))	0.10	3.7(1)
O4	16n	(0.6352(2), 0.5, 0.6059(1))	0.11	3.7(1)

Table S9 The details of the crystal structure of $\text{Bi}_4(\text{V}_{0.9}\text{Cu}_{0.1})_{1.85}\text{O}_{10.3475}$ obtained from PXRD

$\text{Bi}_4(\text{V}_{0.9}\text{Cu}_{0.1})_{1.85}\text{O}_{10.3475}$ (from PXRD)				
Space group		$I4/mmm$ (NO.139)		
a (Å)		3.9366(4)		
c (Å)		15.4678(1)		
V (Å ³)		239.715(2)		
d_{theory} (g cm ⁻³)		7.60(2)		
Atom	Site	Coordinate	Occ.	B_{iso} (Å ²)
Bi	4e	(0.5, 0.5, 0.1679(4))	1	2.1(1)
V	2a	(0, 0, 0)	0.8325	0.8(1)
Cu	2a	(0, 0, 0)	0.0925	0.8(1)
O1	4d	(0, 0.5, 0.25)	1	3.9(1)
O2	8g	(0.5, 0, 0.4797(2))	0.50	8.0(1)
O3	4e	(0, 0, 0.1116(1))	0.1	6.0(1)
O4	16n	(0.6352(2), 0, 0.6059(1))	0.12	6.0(1)

Table S10 The details of the crystal structure of $\text{Bi}_4(\text{V}_{0.9}\text{Cu}_{0.1})_{1.90}\text{O}_{10.465}$ obtained from PXRD and SRXRD

$\text{Bi}_4(\text{V}_{0.9}\text{Cu}_{0.1})_{1.90}\text{O}_{10.465}$ (from PXRD and SRXRD)				
Space group		$I4/mmm$ (NO.139)		
a (Å)		3.9349(4)		
c (Å)		15.4762(1)		
V (Å ³)		239.626(2)		
d_{theory} (g cm ⁻³)		7.64(2)		
Atom	Site	Coordinate	Occ.	B_{iso} (Å ²)
Bi	4e	(0.5, 0.5, 0.1685(4))	1	1.9(1)
V	2a	(0, 0, 0)	0.855	1.5(1)
Cu	2a	(0, 0, 0)	0.095	1.5(1)
O1	4d	(0, 0.5, 0.25)	1	3.5(1)
O2	8g	(0.5, 0, 0.4789(2))	0.45	8.0(1)
O3	4e	(0, 0, 0.1102(1))	0.13	3.0(1)
O4	16n	(0.6497(2), 0.5, 0.6017(1))	0.14	3.0(1)

Table S11 The details of the crystal structure of $\text{Bi}_4(\text{V}_{0.9}\text{Cu}_{0.1})_{1.95}\text{O}_{10.5825}$ obtained from PXRD and PND

$\text{Bi}_4(\text{V}_{0.9}\text{Cu}_{0.1})_{1.95}\text{O}_{10.5825}$ (from PXRD and PND)				
Space group		$I4/mmm$ (NO.139)		
a (Å)		3.9243(4)		
c (Å)		15.4558(1)		
V (Å ³)		238.092(2)		
d_{theory} (g cm ⁻³)		7.72(2)		
Atom	Site	Coordinate	Occ.	B_{iso} (Å ²)
Bi	4e	(0.5, 0.5, 0.1685(4))	1	2.7(1)
V	2a	(0, 0, 0)	0.9	0.2(1)
Cu	2a	(0, 0, 0)	0.1	0.2(1)
O1	4d	(0, 0.5, 0.25)	1	2.6(1)
O2	8g	(0.5, 0, 0.4720(2))	0.38	8.9(1)
O3	4e	(0, 0, 0.1102(1))	0.27	4.2(1)
O4	16n	(0.6955(2), 0.5, 0.5965(1))	0.15	4.2(1)

Table S12 The details of the crystal structure of $\text{Bi}_4(\text{V}_{0.9}\text{Cu}_{0.1})_{2.00}\text{O}_{10.7}$ obtained from PXRD and PND

$\text{Bi}_4(\text{V}_{0.9}\text{Cu}_{0.1})_{2.00}\text{O}_{10.7}$ (from PXRD and PND)				
Space group		$I4/mmm$ (NO.139)		
a (Å)		3.9251(4)		
c (Å)		15.4482(1)		
V (Å ³)		238.003(2)		
d_{theory} (g cm ⁻³)		7.75(2)		
Atom	Site	Coordinate	Occ.	B_{iso} (Å ²)
Bi	4e	(0.5, 0.5, 0.1688(4))	1	1.5(1)
Cu	2b	(0, 0, 0)	0.1	3.1(1)
V	2b	(0, 0, 0)	0.9	3.1(1)
O1	4d	(0, 0.5, 0.25)	1	1.6(1)
O2	8g	(0.5, 0, 0.4760(2))	0.40	5.8(1)
O3	4e	(0, 0, 0.1099(1))	0.25	3.2(1)
O4	16n	(0.6840(2), 0.5, 0.5967(1))	0.15	3.2(1)

Table S13. Structural parameters extracted from quantitative EXAFS curve fitting

Sample	Path	CN	$R(\text{\AA})$	$\sigma^2(\text{\AA}^2)$	$\Delta E_0(\text{eV})$	$R\text{-factor}(\%)$
$x = 1.70$	V–O	2	1.6977	0.002	8.8	1.7
$x = 1.75$	V–O	2	1.7346	0.001	12.1	1.8
$x = 1.80$	V–O	2	1.7187	0.001	10.7	1.0
$x = 1.85$	V–O	2	1.7147	0.001	10.6	0.9
$x = 1.90$	V–O	2	1.7136	0.003	10.3	1.1
$x = 1.95$	V–O	2	1.7144	0.001	10.5	0.8
$x = 2.00$	V–O	2	1.7159	0.002	10.3	1.2

Table S14. Structural parameters extracted from quantitative EXAFS curve fitting

Sample	Path	CN	$R(\text{\AA})$	$\sigma^2(\text{\AA}^2)$	$\Delta E_0(\text{eV})$	$R\text{-factor}(\%)$
$x = 1.70$	Cu–O	4	1.9057(1)	0.003	2.3	0.2
$x = 1.75$	Cu–O	4	1.9041(1)	0.003	2.8	0.2
$x = 1.80$	Cu–O	4	1.9081(1)	0.002	3.7	0.3
$x = 1.85$	Cu–O	4	1.9057(1)	0.001	2.0	0.1
$x = 1.90$	Cu–O	4	1.9054(1)	0.002	3.1	1.3
$x = 1.95$	Cu–O	4	1.9108(1)	0.003	3.4	0.5
$x = 2.00$	Cu–O	4	1.9175(1)	0.003	1.8	0.3